JOURNAL OF MATERIALS SCIENCE **38** (2003) 1479– 1484

Nickel high temperature oxydation under creep loading using acoustic emission monitoring

L. GAILLET, S. BENMEDAKHNE, A. LAKSIMI*‡, G. MOULIN
Laboratoire Roberval, Université de Technologie de Compiègne, UPRESA 6066, BP 20529, 60205 Compiègne, France
E-mail: abdelouahed.laksimi@utc.fr

We have studied the cracking behavior of oxide scales developed on high purity nickel single crystal during creep deformation under oxygen at 550°C. The oxide microstructure exhibits a network of parallel cracks with a constant spacing between cracks. The deterioration of the oxide scale is monitored by acoustic emission. The creep deformation mechanisms with oxide scale are investigated and compared to vacuum creep experiments. Differences in creep behavior between these two atmospheres are obvious. This study is followed by a stress relaxation analysis. The acoustic emission technique provides a large number of results for the understanding of damage of the oxide scales during creep deformation at 550°C.

1. Introduction

Pure nickel or its alloys are well known for their good mechanical properties and corrosion resistance at high temperature in oxidising environments [1]. Nevertheless, application of a mechanical stress to a metallic material during oxidation modifies the protective behavior of its oxide scale [2]. Indeed, strong damage can occur on surface and the natural oxide which isolates metal from the corrosive atmosphere quickly loses its protective properties [3]. These phenomena are induced by growth stresses and can be largely enhanced in the case of applied stress or strain [4]. Synergetic effects between the mechanical deformation and the oxidation are generally a detrimental factor leading to the destruction of materials. But the analysis of this synergy requires the development of specific techniques like mechanical testing in different oxidizing atmospheres. Basing on these techniques, a study was carried out for a better understanding of nickel creep behavior and to investigate the main damage of the oxide scale under oxygen at 550°C.

In this work a new methodology is proposed based on acoustic emission analysis and microscopic observations to follow the chronological appearance, to understand damage behaviour and to assess this methodology as a measure of damage severity of the oxide.

The potential of acoustic emission A.E. for providing reliable information and for its utilisation in service depends largely on the A.E. instrumentation available [5]. Significant improvements and modifications have been made in acoustic emission systems including features for numerical data acquisition and analyses. It also allows different types of detection and location of defects, amplitude analysis, energy and duration analysis, counts, counts to peak and frequency analysis, which are coupled with data acquisition systems to display the information in real-time [6]. The more numerical modern systems, coupled with qualified mechanical analysis of materials, enable determination not only of the occurrence of damage, but also the type and extent of damage mechanisms.

2. Material and experimental procedure

Plate specimens were extracted from a single crystal (111) of nickel bar of high purity (residual content of impurities lower than 30 ppm) prepared by Johnson Matthey Comp. These specimens were machined to obtain a rectangular useful length of 12 mm, a width of 2 mm and a thickness of 1 mm. Annealing was performed for 5 hours in a primary vacuum, improved by an oxygen trapping system, at 900°C.

A specific device was developed which made it possible to apply a mechanical load in a controlled atmosphere (16-oxygen, 18-oxygen, vacuum) to the sample [7]. The samples are tightened in a pair of alumina tongs. The force is measured by a force sensor located in the internal part of the rod near the cooled side. The force is maintained constant by continuous displacement between the two tongs, which is determined by an elongation sensor put at the outer end of the alumina rod. This set-up enables the measurement of the stresses and strains induced during oxidation of nickel with or without mechanical loading (Fig. 1). An

*Author to whom all correspondence should be addressed.
‡*Present Address*: Département de Génie Mécanique, Laboratoire Roberval, Université de Technologie de Compiègne, UMR 6066 du CNRS, B.P. 20529–60206 Compiègne cedex, France.

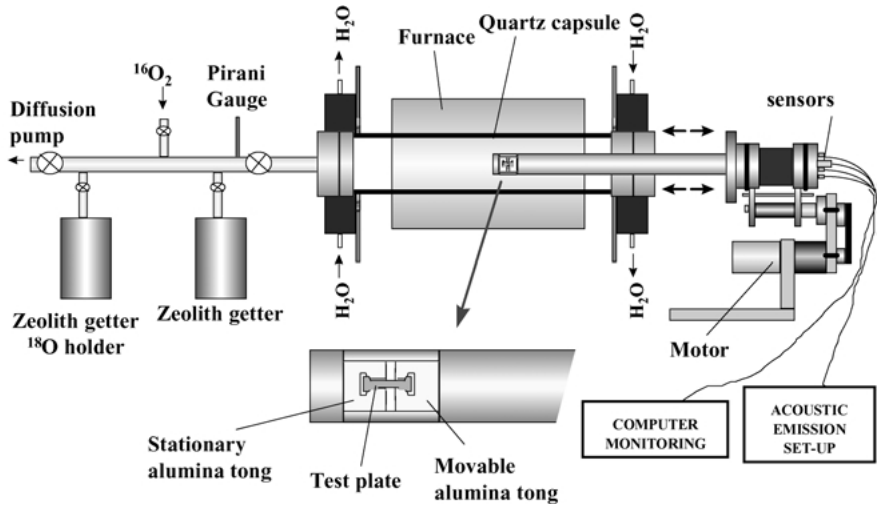

Figure 1 Schematic of the deformation-oxidation test set-up with Acoustic Emission equipment.

oxygen isotope (^{18}O) was chosen to study the diffusion of oxygen but results obtained by this technique are not dealt with this article [8].

The experimental procedure was as follows: the samples were initially preoxidized without any load during 4 hours at 550°C under oxygen pressure of 10^5 Pa. They were then deformed in creep under the same conditions of oxidation with loads varying from 15 to 60 MPa. For the test-specimens tested in vacuum, the same experimental process was used again only that the oxidizing atmosphere was replaced with vacuum.

The acoustic emission system used in this study consisted of the Physical Acoustics Corporation System Model AEDSP-32/16 & MISTRAS 2001. The sampling of features is 2 at 10 MHz per channel, with lower noise (<18 dB threshold) and the CPU selectable, 15 filters/channel (LP, HP, BP). The (2/4/6/) preamplifier was used with the A.E. system, with power supplied via the output signal BNC. In our case the gain was 40 dB and the plug-in filter was band pass (20 and 1200 kHz). Acoustic Emission signals were detected using a piezoelectric transducer in a large range of frequencies from 200 kHz to 1 MHz. A coupling fluid was used to have a flawless contact between the transducer and the specimen support.

3. Microstructural study

The oxide scale exhibits, after 4 hours of preoxidation, a duplex structure. The oxidized layer is composed of large columnar grains in the outer zone and of small equiaxed grains in the inner zone [9]. The oxide scale thickness is 0.4 μm for the outer scale and nearly 0.1–0.2 μm for the inner one, after oxidation for 4 h at 550°C in oxygen. The two layers have the same composition and structure, i.e., NiO. The mean radius of NiO grains of the external layer is between 100 to 200 nm. After the nickel samples have been tested in creep, in oxygen, at 550°C, a network of parallel cracks has been developed on the surface of the oxide scale with an orientation perpendicular to the tensile strain axis (Fig. 2).

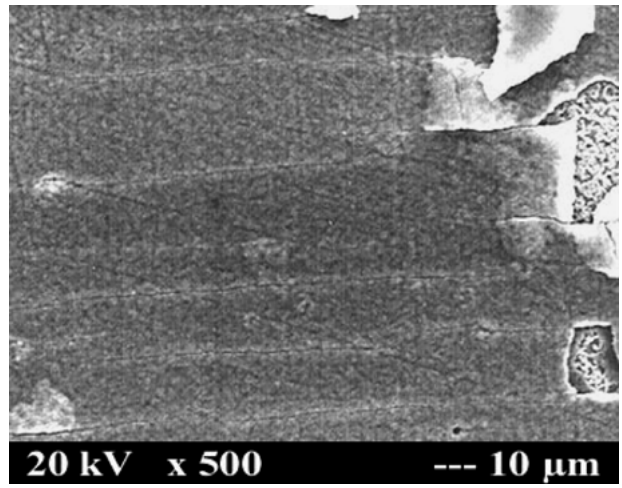

Figure 2 Periodic cracking of the oxide scale of nickel tested in creep at 550°C with a stress of 25 MPa (Scanning electron microscopy).

Such an array of cracks was already observed by many authors [10, 11]; it appears when the applied stress exceeds a critical stress for oxide failure by cracking:

$$\sigma_c = K_{IC}/f(\pi c)^{1/2}$$

where σ_c is the critical stress, K_{IC} is the critical stress intensity factor, f denotes a geometric factor ranging between 2 and 4, and c is the defect half length. The nature of defect c is mainly associated with cracks and its size is about 10 μm.

The critical stress for these cracks is nearly 10 MPa. The spacing between the cracks decreases when the applied load increases. Many oxide buckling and spallation are generated at the highest stresses (Fig. 3).

4. Mechanical study

To highlight possible synergetic effects involving reactivity of surface and mechanical evolution in creep, the mechanical behavior observed in vacuum and under oxygen needs be examined.

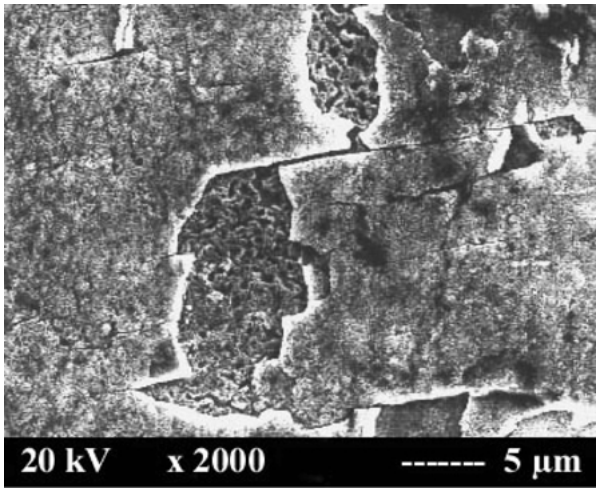

Figure 3 Spallation of the outer scale of NiO for an applied stress of 35 MPa under oxygen at 550°C.

Under vacuum, the variation of the strain rate versus the applied stress corresponds with a Harper-Dorn creep [12] (Fig. 4). Indeed, this creep behavior is found to be active when the dislocation density, due to the (111) glide systems, is low (low creep load). Then, the deformation rate is nearly proportional to the applied stress (slope $n = 1.4$).

For low stresses under oxygen, the deformation mechanism in temperature (slope $n = 1.2$) is similar to nickel in vacuum (slope = 1.45) (Fig. 4). At higher stresses, a power law creep is now established ($n = 4$). A mechanism of deformation concerning the dislocations movement is evidenced with a power exponent n found equal to 4, i.e., a value not very far from the data of 3.5 or 3.8 that are reported for nickel in the study of H. Siethoff *et al.* [13].

The deformation behavior of oxidized nickel samples is complex. Two distinct phases, nickel and oxide are present and they deform by elasticity and creep. More information on the mechanical behaviour of such a complex oxidised system has been collected with the help of stress relaxation experiments. The stress relaxation after creep was studied by stopping the elongation of the sample and recording the isothermal evolution of the applied stress. The stress relaxation analysis is based

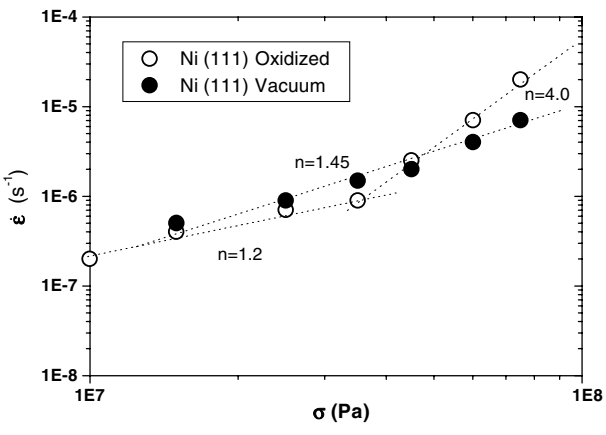

Figure 4 Logarithm of the strain rate (ln ($\dot{\varepsilon}$)) versus the logarithm of stress (ln (σ)) for creep in vacuum or in oxygen.

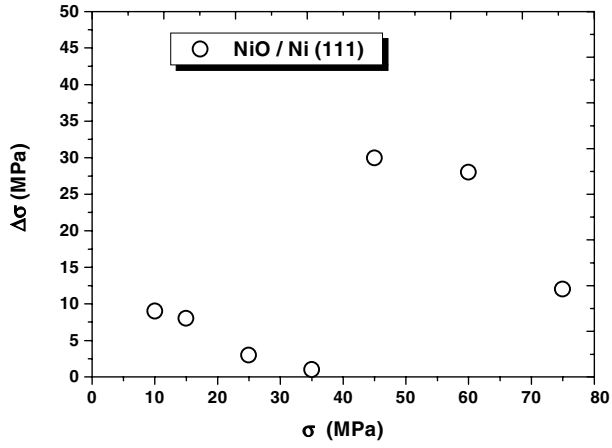

Figure 5 Variation of the relaxed stress $\Delta\sigma$ with the applied stress σ after creep deformation under oxygen for a Ni/NiO system at 550°C.

on the sharing of applied stress into two components, the relaxed stress (or $\Delta\sigma$) and the internal stress (or σ_i) [14].

$$\sigma_{\text{applied}} = \Delta\sigma + \sigma_i$$

The relaxed stress for the oxidised sample corresponds to a mechanism of elastic energy relief used for the displacement of moving dislocations. For deformation occurring by interface sliding, this energy enables dislocations to jump over obstacles of small size and controls the kinetics of deformation. This process is thermally activated [15]. The internal stress is in relation with the long distance displacement of dislocations. This displacement is hampered by dislocation interactions, grain-boundaries, and all defects contributing to hardening.

In the present study, we only consider the relaxed stress plotted as function of the applied stress (Fig. 5).

There is a linear decrease of the relaxed stress with the applied stress for low stresses above a critical applied stress (35–45 MPa), the relaxed stress that becomes significant again, also follows a decrease versus external stress. This behavior is not evidenced in the case of relaxation tests on bare nickel single crystals (with a continuous increase of $\Delta\sigma$). The dislocation motion seems fast for the lowest stresses, which permits fast stress relaxation. This behavior would be related to the fact that the outer oxide scale is cracked in the initial stage of the deformation, so that dislocations are not strongly constrained in their movement towards the surface. But with increasing load, microstructural effects may be possible, like healing of the scale. This continuous new film would then inhibit the elimination of dislocations and the values of $\Delta\sigma$ decrease when stresses become higher. At a critical applied stress level, some cracks appear in the inner oxide scale. That is shown on the stress relaxation curves by a sharp increase of $\Delta\sigma$ 45 MPa).

5. Acoustic emission study

The creep experiments at 550°C on nickel test-specimens under vacuum and oxygen can be subdivided

in three distinct steps. The first phase is 4 hours vacuum annealing or a preoxidation according to the device atmosphere. The second one is creep itself with a duration of approximately 2.5 h, it breaks up into two domains according to the reactive atmosphere (oxygen ^{16}O, then oxygen ^{18}O). The last phase is the stress relaxation (constant total strain) for about one hour (Fig. 6). The information gained from the acoustic emission during these different phases will be detailed now.

During the preoxidation stage under oxygen or vacuum annealing, the acoustic activity is not very significant with a low number of hits that appear in a discontinuous way. The intensity of the acoustic events and their number is almost identical for the two atmospheres; thus this acoustic emission is attributed only to problems of the installation to achieve equilibrium in temperature. During this stage, the system consisting of the test-specimens (nickel) and the device designed for creep (alumina parts) reach thermal equilibrium from the ambient temperature to 550°C. The positioning of the test-specimens in the alumina machine grips proceeds in the same time. Mechanical and thermal stability is achieved at the end of 4 hours period. During the stage of stress relaxation, there are no (or few) acoustic events. Therefore, we will only focus on the acoustic activity during creep changes according to the atmosphere used (vacuum/oxygen).

First of all, we must be sure that collected acoustic emission signals are those emitted by the NiO oxide scale. Under vacuum, the number of events is low and almost negligible. Under oxygen, a significant generation of A.E. is observed during primary creep. This acoustic activity continues during secondary creep. Owing to the fact that acoustic activity is low under vacuum, it appears clearly that evolution of the oxide layer takes place during creep.

Analyzing the A.E. signals during the creep stage, the A.E. activity during this stage was found to be very significant in terms of amplitude and energy. This can be attributed to the cracks generation at the first stages of creep [11, 16]. Microstructural studies, like S.E.M. (scanning electron microscopy), confirm the creation of cracks at this stage, which can be explained by a mechanical model already presented. During the secondary creep stage, A.E. activity is evidenced but the number of events and their intensities are lower than the first stage. Indeed, cracks evolve with the deformation rate; buckling and spallation of the oxide scale appear during deformation as evidenced by other authors [17].

These different mechanisms of oxide scale damage can be separated with the acoustic emission technique. For example, the A.E. energy parameter can be used for identifying these mechanisms (Fig. 7).

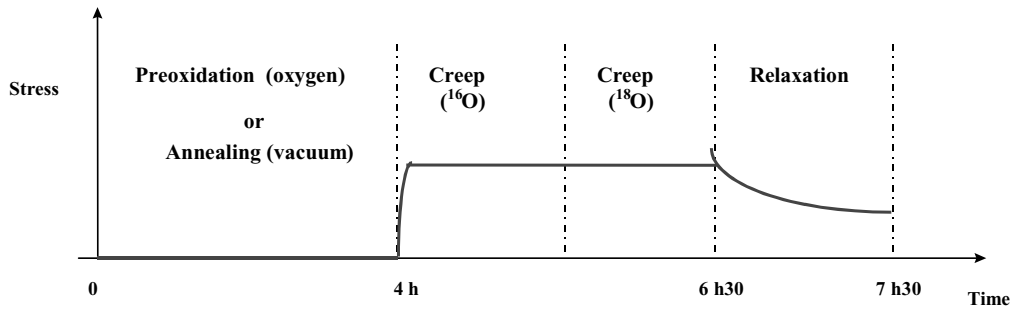

Figure 6 The different steps in creep experiments.

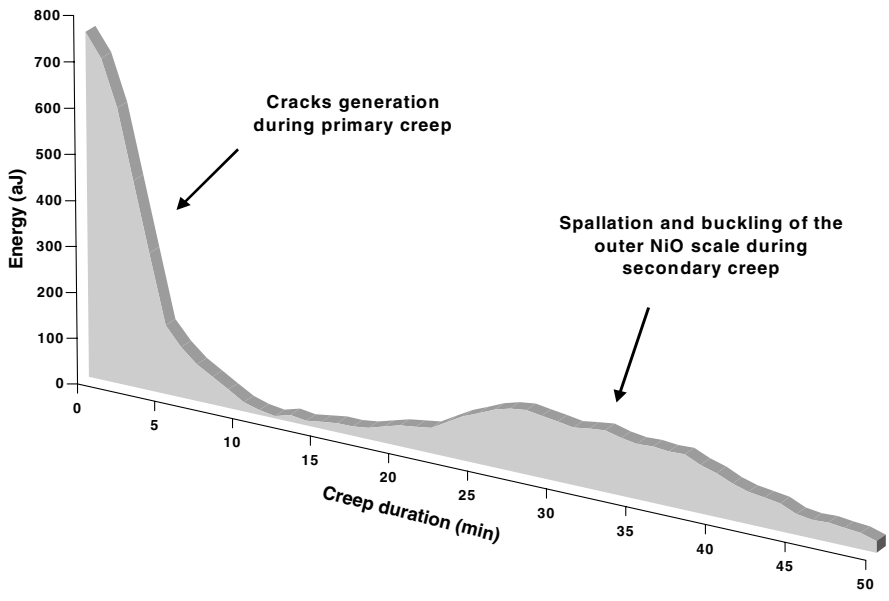

Figure 7 Acoustic emission identification of the different damage types that occur in the outer NiO scale during creep deformation.

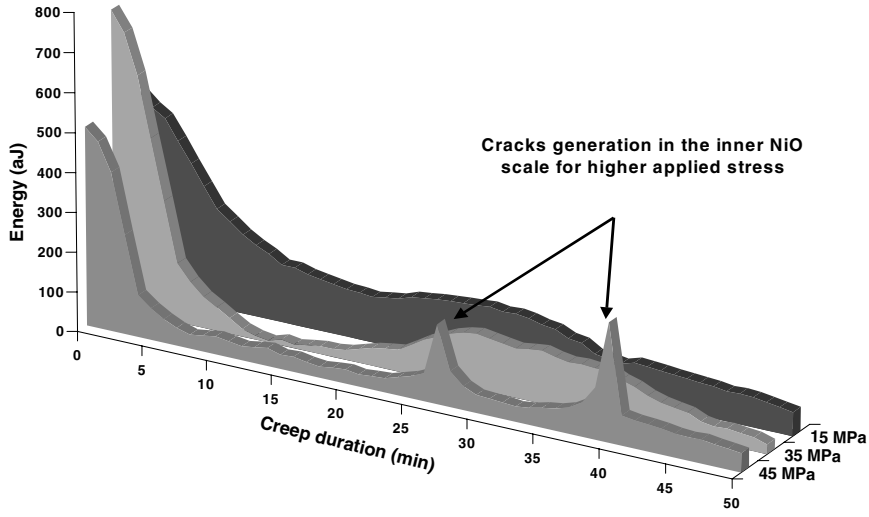

Figure 8 Evolution of the acoustic emision energy (attoJoule) versus duration of creep for several levels of applied stress.

During creep deformation, the first damage takes place by a crack generation in the external scale, appearing few minutes after applying a load to the test-specimen. This damage is accompanied by A.E. events with a high energy. The second phenomenon is the destruction of the outer scale of NiO by spallation and buckling, which is characterized by a lower energy for A.E. events and a long time duration of A.E. signal. This is a general observation for the Ni/NiO samples tested in creep under oxygen at 550°C. These experimental results require a better understanding of the microstructure mechanisms in term of energy. As mentioned recently by authors, the energy for spallation and buckling mechanisms can corresponds not to classical interfacial bonding energy but to oxide cohesion energy. This can explain the weaker value of energy for scales debonding than for cracking. It should be also observed that acoustic energy is not directly related to the total energy of damage mechanisms and represents only a part of this latter.

A second step is to study the evolution of the oxide scale damage (new phenomena or enhancement) with increasing creep deformation. The damage severity is not really directly proportional to the stress intensity. Depending to the applied stress, the crack generation can release energy, noticed by the A.E. system, with higher or lower acoustic energy according the applied load (Fig. 8). The strength of the external scale damage (buckling, spallation) also depends on the applied stress. The most important fact is the possibility of crack generation in the inner NiO scale for a critical applied stress domain (35–45 MPa). This result is confirmed by the relaxation and global creep tests that exhibit a change of slope precisely in this range Since the outer scale of NiO is largely damaged for these stresses, only the cracking of inner one can explain these mechanical behaviors.

The acoustic emission thus confirms the results observed in microstructural and mechanical studies. Indeed, it is observed that cracking takes place and that oxide scale degradation appears for large stresses. In the stress relaxation study, the change of slope is precisely noticed at 45 MPa, which could be explained by the cracking of the internal oxide scale. These first results are promising and require more accurate analysis. Thus, establishing a failure criterion like the fracture toughness (K_{1c}) for oxide scales appears possible by a combined use of acoustic emission and with a thorough analysis of the nature of the defects produced.

6. Conclusion

The creep study under oxygen and in vacuum at 550°C indicates differences in mechanical behavior of Ni specimens tested that can be attributed to the presence of the oxide scale on the surface of the metal. Stress relaxation experiments can be helpful for the understanding of such a complex metal-oxide system, describing the true stress operating during deformation. After deformation, the oxide microstructure exhibits a network of parallel cracks and numerous spallations. This failure behavior is confirmed by *in-situ* acoustic emission, which allows continuous monitoring of damage generation and evolution during creep tests. Most types of damage encountered can be identified using this technique. This type of analysis highlights the potential of acoustic emission as a complementary technique for studying material degradation in high temperature corrosion.

References

1. J. F. STRINGER, "High Temperature Corrosion of Aerospace Alloys," NATO series, AGARDograph 200, 1975, p. 117.
2. G. MOULIN, C. MONS, C. SEVERAC, C. HAUT, G. RAUTUREAU and E. BEAUPREZ, *Oxid. Met.* **40** (1993) 85.
3. P. KOFSTAD, "High Temperature Corrosion" (Elsevier Applied Science, London, 1988).
4. G. MOULIN, P. AREVALO and A. SALLEO, *Oxid. Met.* **45** (1996) 153.
5. A. LAKSIMI, S. BENMEDAKHENE and L. BOUNOUAS, in Proceedings of ICCM 12, Paris, July 1999.
6. X. L.GONG, A. LAKSIMI and M. L.BENZEGGAGH, *Revue des Composites et des Matériaux Avancés* **8** (1998) 7.
7. G. MOULIN and F. MAUREL, in Proceedings of the Fourth European Conference on Residual Stresses, Cluny, June 4–6, 1996, edited by S. Denis, J. L. Lebrun, B. Bourniquel, M. Barral and J. F. Flavenot (Paris, 1996) p. 537.
8. P. BERGER, G. MOULIN and M. VIENNOT, *Nucl. Instr. Meth. Phys. Res.* B **130** (1997) 717.

9. H. V. ATKINSON, *Oxid. Met.* **5** (1985) 177.
10. P. HANCOCK and J. R. NICHOLLS, *Mater. Sci. Tech.* **4** (1988) 398.
11. M. NAGL, W. T. EVANS, D. J. HALL and S. R. J SAUNDERS, *J. Phys. 3* **C9** (1993) 933.
12. H. J. FROST and M. F. ASHBY, "Deformation Mechanism Map" (Pergamon Press, Headington Hill Hall, 1982).
13. H. SIETHOFF, W. SCHRÖTER and K. AHLBORN, *Acta Met.* **33** (1985) 443.
14. M. D. DUONG, PhD thesis, Université Pierre et Marie Curie, Paris, 1977.
15. G. BAUR and P. LEHR, CNRS report No. RCP 244, CNRS Vitry (1980).
16. M. NAGL, W. T EVANS, S. R. J SAUNDERS and D. J HALL, in Proceedings of NACE Conference on Life Prediction of Corrodible Structures, Houston, 1992.
17. M. SCHÜTZE, "Protective Oxides Scales and Their Breakdown" (John Wiley & Sons, London, 1997).

Received 26 March
and accepted 21 November 2002